Theory of a Strip-Line Cavity for Measurement of Dielectric Constants and Gyromagnetic-Resonance Line-Widths*

R. A. WALDRON†

Summary—The cavity consists of a half-wavelength or wavelength of strip-line, short-circuited at both ends, and open along the sides. For measurements of dielectric and magnetic properties of samples, it has two apparent advantages over the more usual coaxial line method: the sample is simpler in shape, and it can be inserted without dismantling the cavity. Perturbation formulas are obtained for the frequency shift and change of "Q" on inserting a sample into a position of zero electric or zero magnetic field. The "Q" of the cavity in the absence of a sample is calculated by a perturbation method. The limiting sample size for a given accuracy to be obtained is also discussed.

I. Introduction

IN THE RANGE of frequencies from about 100 Mc to about 2000 Mc, the dielectric constants of materials are usually measured by inserting into a coaxial line a sample of the material in the form of a tube, filling the space between the conductors.[1] Great care is necessary in preparing a sample, for the shape is complicated and the fit must be very good. This difficulty is accentuated if the material is available in the form of a thin sheet from which a number of disks have to be cut and stacked together. To insert the sample, the circuit must be broken, and this introduces the possibility of error because the junction at the break may not be made in exactly the same way after the break as before.

To overcome these difficulties, it was suggested[2] that a strip-line resonator, short-circuited at both ends and open along its sides, be used. Much simpler sample shapes can then be used, and fewer dimensions need to be accurately made to specified values. Also, the sample can be inserted through the open side of the resonator without otherwise disturbing the apparatus. The author has made a study of the relevant theory which forms the subject of the present paper.

By placing a sample in a region of zero magnetic field and maximum electric field, a measurement of dielectric constant can be made. For a cavity half a wavelength long, such a position occurs at the center of the cavity. Measurements of magnetic properties can be made by placing the sample in a position of maximum magnetic and zero electric field. For a half-wavelength cavity, this is at the end of the cavity, and the effect of reflection of the sample in the end wall must be considered.

The field configuration in the cross section of a strip-line is very complicated, and the problem cannot be handled directly in terms of this model. To obtain the problem in a tractable form, the actual strip-line cross section must be mapped into a rectangle, two opposite sides of which correspond to the live strip and one ground plane. This parallel-plate model can then be treated conveniently, and the results obtained for this can be changed by means of the mapping function into those proper to the actual strip-line. Thus the mapping is central to the whole subject of the paper and will be treated first, in Section II. The possibility of mapping in this way depends on the fact that we take the strip-line to be working in its transmission-line mode, in which both the electric and magnetic fields are transverse.

The imaginary part of a dielectric constant or permeability is measured by observing the change of "Q" on inserting the sample. To ensure that measurable values can be obtained, it is necessary to know the "Q" of the unperturbed cavity, and this quantity must be taken into account in designing a cavity. For this reason, a calculation had been made of the "Q" in Section III, using perturbation theory.

Section IV deals with the frequency shift and change of "Q" on inserting a dielectric material into a position of zero magnetic field. This study falls into two parts, the derivation of a formula for the frequency shift in terms of the dielectric constant of the sample and the geometry of the sample and cavity, and an estimate of the maximum dimensions the sample may have if a given accuracy is to be achieved.

The substances on which magnetic measurements will be performed will usually be ferrites, and here the interest is in the diagonal and off-diagonal elements of the permeability tensor and the gyromagnetic-resonance line-width. By placing the sample in different positions, it is possible to measure both elements of the permeability tensor. Only one measurement is necessary to determine the linewidth.

At the center of the common area of two crossed strip-lines, there will be circular polarization, and, by reversing the sense of this, both permeability elements may be measured on a sample placed at this position;

* Received August 2, 1953; revised manuscript received October 7, 1963.

† Research Division, The Marconi Company, Ltd., Great Baddow, Essex, England.

[1] M. Wind and H. Rapaport, Eds., "Handbook of Microwave Measurements," Polytechnic Institute of Brooklyn, N. Y., p. 10.7; 1954.

[2] By the author's colleague, Miss S. P. Maxwell.

this has been suggested by Ogasawara and Shikata.[3] The difficulty here, however, is to relate the frequency shift to the properties; this will be very difficult mathematically—it is not a case of merely extending the theory given in the present paper—and the problem is not solved by Ogasawara and Shikata.

II. Mapping

Fig. 1 shows the cross section of the strip-line. By virtue of the two planes of symmetry, we need consider in detail only one quadrant; the others will follow automatically. We are concerned with the electric field distribution inside the polygon $PQRSTP$, where P is taken to be at infinity. The ground planes will, of course, only be of finite extent, but we assume this extent to be such that, at the edges the energy density is so small that the difference between the actual ground planes and infinite ground planes is negligible.

The mapping is carried out in two stages. First we shall map the polygon $PQRSTP$ of Fig. 1 onto the first quadrant of the ζ plane (Fig. 2) in such a way that the periphery of the polygon in the z plane lies on the real and imaginary axes in the ζ plane. The second stage is to map the first quadrant of the ζ plane onto the interior of a rectangle in the Z plane (Fig. 3). The two transformations are to be carried out in such a way that the two conducting surfaces are on opposite sides of the rectangle in Fig. 3, and occupy the whole of each side. The mapping function we shall use will be doubly periodic in the Z plane, so that if the plane is imagined to be filled with a doubly infinite number of rectangles lying adjacent to one another, the mapping function we shall use can, by suitably choosing certain arbitrary constants, be made to map any quadrant of the ζ plane onto any rectangle in the Z plane. The presence of these alternative rectangles on either side of the one we are concerned with means that the electric lines of force in the Z plane do not go outside the rectangle; they are straight, parallel to the imaginary axis—we have a parallel-plate condenser with no edge effects. From our knowledge of the field distribution in this simple situation, we can deduce certain facts we will need to know about the field distribution in the z plane.

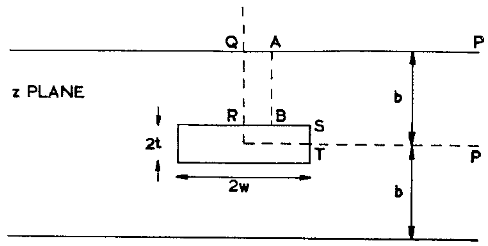

Fig. 1—Cross section of the strip-line.

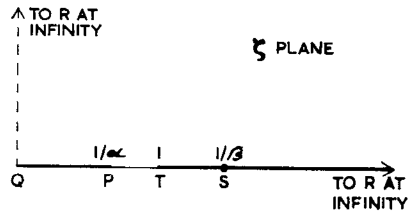

Fig. 2—Mapped form of Fig. 1 (intermediate stage).

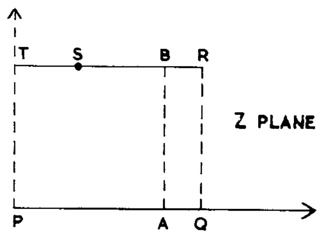

Fig. 3—The strip-line mapped onto a parallel-plate line.

A. z to ζ Mapping

The mapping function is

$$z = z_0 + \lambda \int_0^{\zeta} \frac{1}{1-\alpha^2\zeta^2}\sqrt{\frac{1-\beta^2\zeta^2}{1-\zeta^2}}\, d\zeta \tag{1}$$

where z_0 is a constant to be determined. This is a modified Schwarz-Christoffel transformation. Eq. (1) takes different forms for different ranges of values of ζ. It will be sufficient for our purpose to note the various forms for points on the axes of the ζ plane, corresponding to the perimeter of the polygon in the z plane.

On the line PQ, (1) becomes

$$z = jb + \lambda\{(\beta^2/\alpha^2)F(\phi_1, \beta) + (1 - \beta^2/\alpha^2)\Pi(\phi_1, \alpha^2, \beta)\} \tag{2}$$

where F and Π are incomplete elliptic integrals of the first and third kinds, respectively, and $\sin \phi_1 = \zeta$.

At Q,

$$\zeta = 0, \quad \phi_1 = 0, \quad \text{and} \quad z = jb. \tag{3}$$

At P,

$$\zeta = 1/\alpha \quad \text{and} \quad z = jb + \frac{\lambda\infty}{\alpha}\sqrt{\frac{\alpha^2-\beta^2}{\alpha^2-1}}. \tag{4}$$

On the line PT, (1) becomes

$$z = w + \frac{\lambda(1-\beta^2)}{\alpha^2-1}\Pi\left(\phi_2, \frac{\alpha^2-\beta^2}{\alpha^2-1}, \beta\right) \tag{5}$$

where

$$\sin\phi_2 = \sqrt{(1-\zeta^2)/(1-\beta^2\zeta^2)}.$$

At P,

$$\zeta = 1/\alpha, \quad \text{and} \quad z = \frac{\lambda\infty}{\alpha}\sqrt{\frac{\alpha^2-\beta^2}{\alpha^2-1}}. \tag{6}$$

At T,

$$\zeta = 1, \quad \phi_2 = 0, \quad \text{and} \quad z = w. \tag{7}$$

[3] N. Ogasawara and Y. Shikata, "Improved permittivity and permeability measurements," *Microwaves*, vol. 1, pp. 20–23; October, 1962.

On the line TS, (1) becomes

$$z = w - j\lambda \left\{ F(\phi_3, \beta') - \frac{\alpha^2 - \beta^2}{\alpha^2 - 1} \Pi\left(\phi_3, \frac{1-\beta^2}{1-\alpha^2}, \beta'\right) \right\} \quad (8)$$

where

$$\sin \phi_3 = \sqrt{(1 - 1/\zeta^2)/(1-\beta^2)}, \quad \text{and} \quad \beta' = \sqrt{1-\beta^2}.$$

At T,

$$\zeta = 1, \quad \phi_3 = 0, \quad \text{and} \quad z = w. \quad (9)$$

At S,

$$\zeta = 1/\beta, \quad \phi_3 = \pi/2,$$

and

$$z = w - j\lambda \left\{ K(\beta') - \frac{\alpha^2 - \beta^2}{\alpha^2 - 1} \Pi\left(\frac{1-\beta^2}{1-\alpha^2}, \beta'\right) \right\}. \quad (10)$$

On the line SR, (1) becomes

$$z = jt + \lambda\{F(\phi_4, \beta) - (1 - \beta^2/\alpha^2)\Pi(\phi_4, \beta^2/\alpha^2, \beta)\} \quad (11)$$

where $\sin \phi_4 = 1/\beta\zeta$.
At S,

$$\zeta = 1/\beta, \quad \phi_4 = \pi/2,$$

and

$$z = jt + \lambda\{K(\beta) - (1 - \beta^2/\alpha^2)\Pi(\beta^2/\alpha^2, \beta)\}. \quad (12)$$

At R,

$$\zeta = \infty, \quad \phi_4 = 0, \quad \text{and} \quad z = jt. \quad (13)$$

On the line RQ, (1) becomes

$$z = jb + j\lambda \left\{ \frac{1-\beta^2}{\alpha^2 - 1} F(\phi_5, \beta') - \frac{\alpha^2 - \beta^2}{\alpha^2 - 1} \Pi(\phi_5, 1 - \alpha^2, \beta') \right\} \quad (14)$$

where

$$\sin \phi_5 = \frac{1}{\sqrt{1 - 1/\zeta^2}} \quad \text{and again} \quad \beta' = \sqrt{1-\beta^2}.$$

At R, $\zeta = j\infty$, $\phi_5 = \pi/2$, and

$$z = jb + j\lambda \left\{ \frac{1-\beta^2}{\alpha^2 - 1} K(\beta') - \frac{\alpha^2 - \beta^2}{\alpha^2 - 1} \Pi(1 - \alpha^2, \beta') \right\}. \quad (15)$$

At Q,

$$\zeta = j0, \quad \phi_5 = 0, \quad \text{and} \quad z = jb. \quad (16)$$

The constants α, β, and λ can be obtained in terms of the geometry of the strip-line, *i.e.*, in terms of w, t, and b. At S,

$$z = w + jt. \quad (17)$$

At R,

$$z = jt. \quad (18)$$

Comparing (10) and (17),

$$t = -\lambda \left\{ K(\beta') - \frac{\alpha^2 - \beta^2}{\alpha^2 - 1} \Pi\left(\frac{1-\beta^2}{1-\alpha^2}, \beta'\right) \right\}. \quad (19)$$

Comparing (12) and (17),

$$w = \lambda\{K(\beta) - (1 - \beta^2/\alpha^2)\Pi(\beta^2/\alpha^2, \beta)\}. \quad (20)$$

Comparing (15) and (18),

$$b = \lambda\left(\frac{\alpha^2 - \beta^2}{\alpha^2 - 1}\right) \cdot \left\{ \Pi\left(\frac{1-\beta^2}{1-\alpha^2}, \beta\right) + \Pi(1-\alpha^2, \beta') - K(\beta') \right\}. \quad (21)$$

It is convenient to deal with t/b and w/b rather than with t and w themselves. Curves of t/b and w/b as functions of α, with β as a parameter, are given in Figs. 4 and 5. α and β are numerical constants, but it is clear from (21) that λ will have the dimensions of b. No advantage is to be obtained by normalizing b, *e.g.*, with respect to the free-space wavelength, so we will retain b as a length. Eq. (21) simplifies to

$$\lambda = \frac{2\alpha b}{\pi}\sqrt{\frac{\alpha^2 - 1}{\alpha^2 - \beta^2}}. \quad (22)$$

B. ζ to Z Mapping

The mapping function is

$$Z = Z_0 + L\int_0^\zeta \frac{d\zeta}{\sqrt{(1-\zeta^2)(1-\alpha^2\zeta^2)}}. \quad (23)$$

This is again a modified Schwarz-Christoffel transformation. As before, this function takes different forms for different ranges of values of ζ. Again, we only need consider the periphery of the rectangle in the Z plane.

On the line QP, (23) becomes

$$Z = K(1/\alpha) + \frac{L}{\alpha} F(\theta_1, 1/\alpha) \quad (24)$$

where

$$\sin \theta_1 = \alpha\zeta.$$

At Q,

$$\zeta = 0, \quad \theta_1 = 0, \quad \text{and} \quad Z = K(1/\alpha). \quad (25)$$

At P,

$$\zeta = 1/\alpha, \quad \theta_1 = \pi/2, \text{ and } Z = K(1/\alpha)[1 + L/\alpha]. \quad (26)$$

But at P,

$$Z = 0. \quad \therefore L = -\alpha. \quad (27)$$

This value of L will be taken in future, so that L will not appear again explicitly.

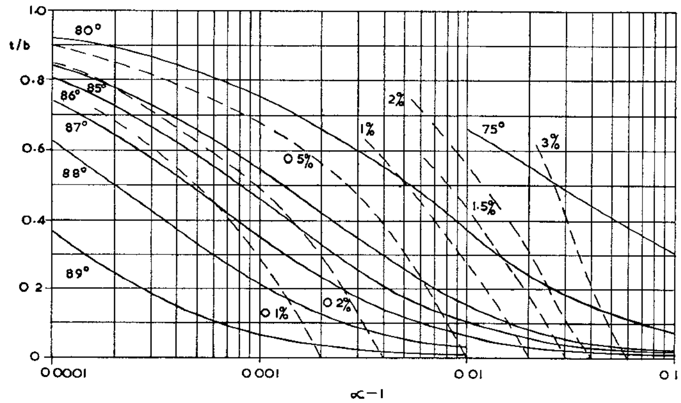

Fig. 4—t/b as a function of α, with β as a parameter. β is the sine of the angle given.

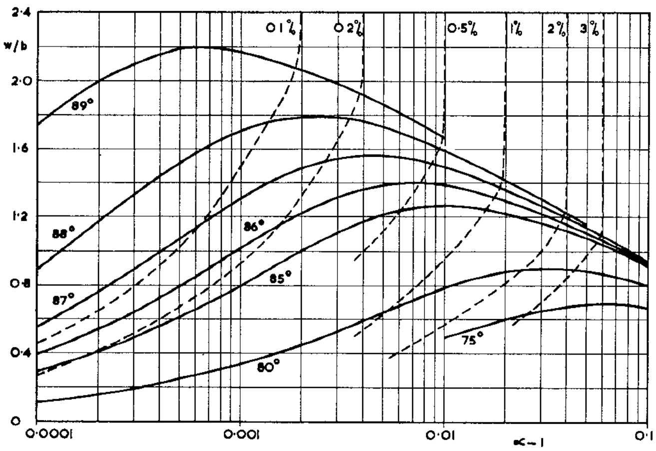

Fig. 5—w/b as a function of α, with β as a parameter. β is the sine of the angle given.

On the line PT, using also (27), (23) becomes

$$Z = jF(\theta_2, \gamma) \tag{28}$$

where

$$\sin\theta_2 = \sqrt{\frac{\alpha^2\zeta^2 - 1}{\zeta^2(\alpha^2 - 1)}} \quad \text{and} \quad \gamma = \sqrt{1 - 1/\alpha^2}.$$

At P,

$$\zeta = 1/\alpha, \quad \theta_2 = 0, \quad \text{and} \quad Z = 0. \tag{29}$$

At T,

$$\zeta = 1, \quad \theta_2 = \pi/2, \quad \text{and} \quad Z = jK(\gamma). \tag{30}$$

On the line TR, using also (27), (23) becomes

$$Z = jK(\gamma) + K(1/\alpha) - F(\theta_3, 1/\alpha) \tag{31}$$

where

$$\sin\theta_3 = 1/\zeta.$$

At T,

$$\zeta = 1, \quad \theta_3 = \pi/2, \quad \text{and} \quad Z = jK(\gamma). \tag{32}$$

At S,

$$\zeta = 1/\beta, \quad \text{and}$$

$$Z = jK(\gamma) + K(1/\alpha) - F(\mathrm{Sin}^{-1}\beta, 1/\alpha). \tag{33}$$

At R,

$$\zeta = \infty, \quad \theta_3 = 0, \quad \text{and} \quad Z = jK(\gamma) + K(1/\alpha). \tag{34}$$

On the line RQ, using also (27), (23) becomes

$$Z = K(1/\alpha) + jF(\theta_4, \gamma) \tag{35}$$

where

$$\sin\theta_4 = \frac{-j\alpha\zeta}{\sqrt{1 - \alpha^2\zeta^2}} \quad \text{and again} \quad \gamma = \sqrt{1 - 1/\alpha^2}.$$

At R,

$$\zeta = j\infty, \quad \theta_4 = \pi/2, \quad \text{and} \quad Z = K(1/\alpha) + jK(\gamma). \tag{36}$$

At Q,

$$\zeta = j0, \quad \theta_4 = 0, \quad \text{and} \quad Z = K(1/\alpha). \tag{37}$$

C. Form of the Field Near RQ

We shall be particularly interested in the lines of force near RQ, because it is into this region that the sample will be introduced. First, we note that for sufficiently small θ and u

$$F(\theta, k) \fallingdotseq \theta + k^2\theta^3/6, \tag{38}$$

$$\Pi(\theta, \chi, k) \fallingdotseq \theta + (2\chi^2 + k^2)\theta^3/6, \tag{39}$$

$$\mathrm{Sin}^{-1} u \fallingdotseq u + u^3/6. \tag{40}$$

Now consider in Fig. 3 the line AB drawn parallel to QR, so that $QA/QP = x$. This line coincides with a line of electric force, and we wish to know where the points A and B will lie in the z plane. At A, we have, from the values given in Section II-B for Z at P and Q,

$$Z = K(1/\alpha)[1 - x]$$

and from (24), using (27) and (38),

$$Z \cong K(1/\alpha) - (\theta_1 + \theta_1^3/6\alpha^2).$$

Comparing these,

$$\theta_1 \cong xK(1/\alpha)[1 - x^2K^2/6\alpha^2]$$

where K means $K(1/\alpha)$. Now, on $\mathrm{Sin}\,\theta_1 = \alpha\zeta$, and we write ζ_A for the value of ζ for the point A. Hence

$$\zeta_A \cong \frac{1}{\alpha}\,\mathrm{Sin}\left\{Kx(1 - K^2x^2/6\alpha^2)\right\}. \tag{41}$$

Similarly, at B, using (31) and (38),

$$\zeta_B \cong \frac{1}{\mathrm{Sin}\left\{Kx(1 - K^2x^2/6\alpha^2)\right\}}. \tag{42}$$

Eqs. (41) and (42) give the points in the ζ plane onto which A and B map. We do not need to know the detailed form of the curve joining them into which the line AB of Fig. 3 maps.

We are now going to map the points A and B onto the z plane. For the point A, using (40), we write

$$\phi_1 \cong \mathrm{Sin}^{-1}\zeta_A \cong \zeta_A + \zeta_A^3/6$$

and using (38) and (39), (2) then becomes

$$z_A \cong jb + \lambda\{\zeta_A + (1 + 2\alpha^2 - \beta^2)\zeta_A{}^3/6\}.$$

Using (41) and expanding the sine in terms of the angle, this becomes

$$z_A \cong jb + \frac{\lambda Kx}{\alpha}\left\{1 + \frac{K^2x^2}{6}(1 - \beta^2/\alpha^2)\right\}. \qquad (43)$$

Similarly,

$$z_B \cong jt + \frac{\lambda\beta Kx}{\alpha^2}\left\{1 - \frac{K^2x^2}{6\alpha^2}(\alpha^2/\beta^2 - 1)\right\}. \qquad (44)$$

Eqs. (43) and (44) are the required expressions for the positions of A and B in the z plane. They will be discussed further in Section IV.

III. Q of the Cavity

The "Q" can be calculated by the use of perturbation theory. For a cavity with perfectly conducting walls filled with a lossless dielectric (*e.g.*, vacuum), the "Q" is infinite, and $1/Q=0$. The change in $1/Q$ on perturbing this ideal cavity to the actual cavity gives the "Q" of the cavity. It will be legitimate to assume the dielectric filling, which will be air, to be lossless. The finite value of the "Q" will then be due to the replacement of perfectly conducting walls by metal walls.

The perturbation formula is[4]

$$\frac{\delta\omega}{\omega}+\frac{j}{2Q_0} = \frac{N}{D} = \frac{\iiint_{V_1}\{(\boldsymbol{E}_1\cdot\boldsymbol{D}_0-\boldsymbol{E}_0\cdot\boldsymbol{D}_1)-(\boldsymbol{H}_1\cdot\boldsymbol{B}_0-\boldsymbol{H}_0\cdot\boldsymbol{B}_1)\}dV}{\iiint_{V_0}\{\boldsymbol{E}_0\cdot\boldsymbol{D}_0-\boldsymbol{H}_0\cdot\boldsymbol{B}_0\}dV} \qquad (45)$$

where $\boldsymbol{E}_0$, $\boldsymbol{D}_0$, $\boldsymbol{H}_0$, and $\boldsymbol{B}_0$ are the fields and inductions in the unperturbed state and $\boldsymbol{E}_1$, $\boldsymbol{D}_1$, $\boldsymbol{H}_1$, and $\boldsymbol{B}_1$ are additional fields and inductions which, added to $\boldsymbol{E}_0$, $\boldsymbol{D}_0$, $\boldsymbol{H}_0$, and $\boldsymbol{B}_0$, give the fields and inductions in the perturbed cavity. By virtue of the symmetry of the figure in the z plane, we need consider only the cavity consisting of the polygon $PQRSTP$ with length l_0 perpendicular to this polygon. The interior of this is the volume V_0. The volume V_1 is the whole of the volume over which perfect conductor is replaced by metal. It will be convenient to perform the calculation for the mapped form of the cavity in Fig. 3 instead of the more complicated form of Fig. 1.

In V_1, $\boldsymbol{E}_0=0$ and $\boldsymbol{B}_0=0$. The numerator of (45) therefore reduces to

$$N = \iiint_{V_1}\{\boldsymbol{E}_1\cdot\boldsymbol{D}_0 + \boldsymbol{H}_0\cdot\boldsymbol{B}_1\}dV \qquad (46)$$

[4] R. A. Waldron, "Perturbation Theory of Resonant Cavities," *IEE Monograph*, No. 373E; April, 1960.

and there will be two parts to this: N_1 due to the length of the stripline and N_2 due to the short-circuiting plates. For N_1, we note that, at the metallic surface, $\boldsymbol{D}_{01}$ is equal to $\boldsymbol{D}_{00}=\epsilon_0\boldsymbol{E}_{00}$, and that $\boldsymbol{D}_{01}$ is also equal to $\epsilon_0\epsilon(\boldsymbol{E}_1+\boldsymbol{E}_{01})$, where the second subscripts 0 and 1 refer to values in V_0 and V_1, respectively. $\boldsymbol{E}_{01}$ is zero. Thus in V_1, $\boldsymbol{E}_1\cdot\boldsymbol{D}_{01}=\epsilon_0\boldsymbol{E}_{00}{}^2\epsilon/$. Also, at the metallic surface $\boldsymbol{B}_1=\mu_0\boldsymbol{H}_{00}$, since a medium of permeability 0 has been replaced by a medium of permeability 1. Hence

$$\boldsymbol{E}_1\cdot\boldsymbol{D}_0 + \boldsymbol{H}_0\cdot\boldsymbol{B}_1 = \frac{\epsilon_0}{\epsilon}E_{00}{}^2 + \mu_0 H_{00}{}^2 \qquad (47)$$

at the surface. Here ϵ is the dielectric constant of the metal, which is very large and imaginary. Since $\epsilon_0\boldsymbol{E}_{00}{}^2=\mu_0H_{00}{}^2$, this makes the first term on the right-hand side very much less than the second. Thus the term in $\boldsymbol{E}_{00}{}^2$ may be dropped.

For the term $\boldsymbol{H}_0\cdot\boldsymbol{B}_1$ in V_1, we have $\boldsymbol{H}_0$ constant over the transverse plane and equal to the value in V_0, because, in the perfect conductor, $\boldsymbol{H}_{01}$ extends to infinity. However, $\boldsymbol{B}_1$ decays exponentially in the metal because of the skin effect. The value of $\mu_0H_{00}{}^2$ in (47) must therefore be multiplied by the factor exp $\{-(1+j)y/\delta\}$, where y is the distance measured upwards from TR or downwards from PQ in Fig. 3, and δ is the skin depth. We have now evaluated the integrand of (46) for N_1. Performing the integration, we obtain

$$N_1 = (1 - j)\delta\mu_0 H_0{}^2 l_0\cdot PQ \qquad (48)$$

where l_0 is the length of the cavity and H_{00} is the RMS value of the magnetic field averaged, that is, over the cavity length, because the field varies cosinusoidally with length.

For the contribution from the ends, we note that at the ends $\boldsymbol{D}_0=\boldsymbol{E}_0=0$. The contribution is again due to the magnetic field parallel to the surface, so that

$$\frac{N_2}{N_1} = \frac{4\cdot PQ\cdot QR}{2\cdot PQ\cdot l_0} = \frac{2\cdot QR}{l_0}. \qquad (49)$$

The factor 4 in the numerator arises as the product of two factors 2, one for the two ends and one because at the ends of the cavity $\boldsymbol{H}_0$ has its peak value, whereas, along the length, we took the RMS value. The factor QR/l_0 is the ratio of the area of the end-plate to that of one of the lengthwise conducting planes in Fig. 3. The factor 2 in the denominator exists because there are two such planes in which dissipation is taking place.

From (48) and (49),

$$N = (1 - j)\delta\mu_0 H_0{}^2 l_0\cdot PQ[1 + 2QR/l_0]. \qquad (50)$$

For the denominator of (45), we note that

$$\iiint_{V_0}\boldsymbol{E}_0\cdot\boldsymbol{D}_0 dV = -\iiint_{V_0}\boldsymbol{H}_0\cdot\boldsymbol{B}_0 dV$$

and hence

$$D = -2\iiint_{V_0}\boldsymbol{H}_0\cdot\boldsymbol{B}_0 dV = -2\mu_0 H_0{}^2 V,$$

i.e.,

$$D = -2\mu_0 H_0^2 \cdot PQ \cdot QR \cdot l_0 \tag{51}$$

where again H_0 is the RMS field. From (50) and (51), we obtain

$$\frac{N}{D} = \frac{\delta\omega}{\omega} + \frac{j}{2Q_0} = \frac{(j-1)\delta}{2QR}[1 + 2QR/l_0],$$

$$\therefore\ Q_0 = \frac{QR}{\delta[1 + 2QR/l_0]}\cdot$$

Mapping back onto the z plane, we find that δ maps to δ and QR to $b-t$. Writing also

$$\delta = \frac{1}{\pi}\sqrt{\frac{\lambda_0}{120\sigma}}$$

where λ_0 is the free-space wavelength and σ is the conductivity of the metal, we finally obtain

$$Q_0 = \frac{\pi(b-t)\sqrt{120\sigma}}{\sqrt{\lambda_0}\{1 + 2(b-t)/l_0\}}\cdot \tag{52}$$

For example, if $\sigma = 6.10^7$, which is about the value for silver, $b = 1/4''$, $t = 1/16''$, $\lambda_0 = 1$ meter, and $l_0 = 50$ cm, Q_0 is found to be 1220.

IV. Measurement of Dielectric Constant

For this purpose, the sample is to be taken as a small block of height $b-t$, its horizontal surfaces fitting flush with the strip and the ground plane, and its other surfaces being vertical. Otherwise, the shape does not matter. Fig. 6 shows half the cavity, with half the sample in place, taking a rectangular block as sample. The dimensions of the block are $b-t$, $2y$, $2l_1$. It will be convenient to calculate the complex frequency shift for this case; the extension to the more general case follows quite easily and will be discussed afterwards.

In Fig. 1, AB is a straight line parallel to QR, with $QA = RB = y$. In Fig. 3, AB is a straight line parallel to QR, with $QA = RB = xK(1/\alpha)$. From (43) and (44), to the first order in x,

$$y \cong \frac{\lambda Kx}{\alpha} \cong \frac{\lambda\beta Kx}{\alpha^2}, \tag{53}$$

and so the line AB of Fig. 1 will map approximately to the line AB of Fig. 3, if β is very near to α. From Fig. 2, $\beta < 1$ and $\alpha > 1$. Therefore β and α must both be very close to 1, and only such values have been considered in Figs. 4 and 5. In Fig. 3, the lines of force are parallel to AB, and it is easy to calculate the perturbing effect of a sample $ABRQ$; this we shall do shortly. If the sample in the z plane had a curved side to fit the mapped lines of force, the perturbing effect would be the same. Since the sample sides are vertical, the perturbing effect will be nearly the same, if the lines of force are nearly vertical, *i.e.*, if β/α is nearly 1. This imposes limits on the values of t/b and w/b that may be chosen, if a given accuracy is to be achieved. The error from this cause depends only on α and β, not on y or on the properties of the sample. Thus it imposes limitations on the design

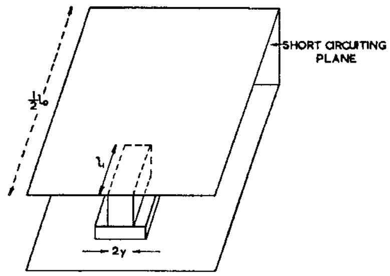

Fig. 6—Placement of the sample for the dielectric-constant measurement. Half the cavity is shown, the remainder being given by reflection in the plane of section.

of the cavity only. Once the cavity has been made, no improvement in accuracy beyond this point can be achieved. The error due to this effect has been estimated roughly, and the dashed curves in Figs. 4 and 5 indicate its value for given values of α and β, and hence of w/b and t/b. For example, if $w/b = 1$ and $t/b = 0.244$, we have $\alpha = 1.012(4)$, $\beta = 0.9911$, and the accuracy is about 1 per cent. This is a limiting figure for the cavity which cannot be improved on by modifying the experimental technique.

We shall now perform the perturbation calculation using the first-order terms in x in (43) and (44) as was done in (53). The terms in x^3 will be required later to estimate the error due to finite sample size. We start from (45), where again V_0 means the volume of the empty cavity, and now V_1 is the sample volume. The sample illustrated in Fig. 6 is asymmetrically placed with respect to the strip. If we consider a quarter of the cavity, as we have been doing, the effect will be the same as if there were two samples above and below the strip. Since in fact there is only one, we must multiply the right-hand side of (45) by one half. In the denominator, the magnetic terms and electric terms make equal contributions to the integral. In the numerator, the magnetic terms vanish because the magnetic field at the position of the sample is zero. Instead of $1/Q_0$, we shall now have the change of $1/Q$, *i.e.*, $1/Q_1 - 1/Q_0$, where Q_0 is the "Q" in the absence of the sample and Q_1 is the "Q" when the sample is introduced. Thus (45) becomes

$$\frac{\delta\omega}{\omega} + \frac{j}{2}\left[\frac{1}{Q_1} - \frac{1}{Q_0}\right] = \frac{\iiint_{V_1}\{\boldsymbol{E}_1 \cdot \boldsymbol{D}_0 - \boldsymbol{E}_0 \cdot \boldsymbol{D}_1\} dV}{4\iiint_{V_0} \boldsymbol{E}_0 \cdot \boldsymbol{D}_0 dV} = \frac{N}{D}\cdot \tag{54}$$

Let us now consider the parallel-plate model of Fig. 3. Then $\boldsymbol{E}_1 = 0$ because the field in the sample is $\boldsymbol{E}_0$. For $\boldsymbol{D}_1$ we have

$$\boldsymbol{D}_0 + \boldsymbol{D}_1 = \epsilon_0\epsilon(\boldsymbol{E}_0 + \boldsymbol{E}_1) = \epsilon_0\epsilon\boldsymbol{E}_0,$$

$$\therefore\ \boldsymbol{D}_1 = \epsilon_0\epsilon\boldsymbol{E}_0 - \boldsymbol{D}_0 = \epsilon_0\epsilon\boldsymbol{E}_0 - \epsilon_0\boldsymbol{E}_0,$$

i. e.,

$$\boldsymbol{D}_1 = \epsilon_0(\epsilon - 1)\boldsymbol{E}_0.$$

Eq. (54) becomes

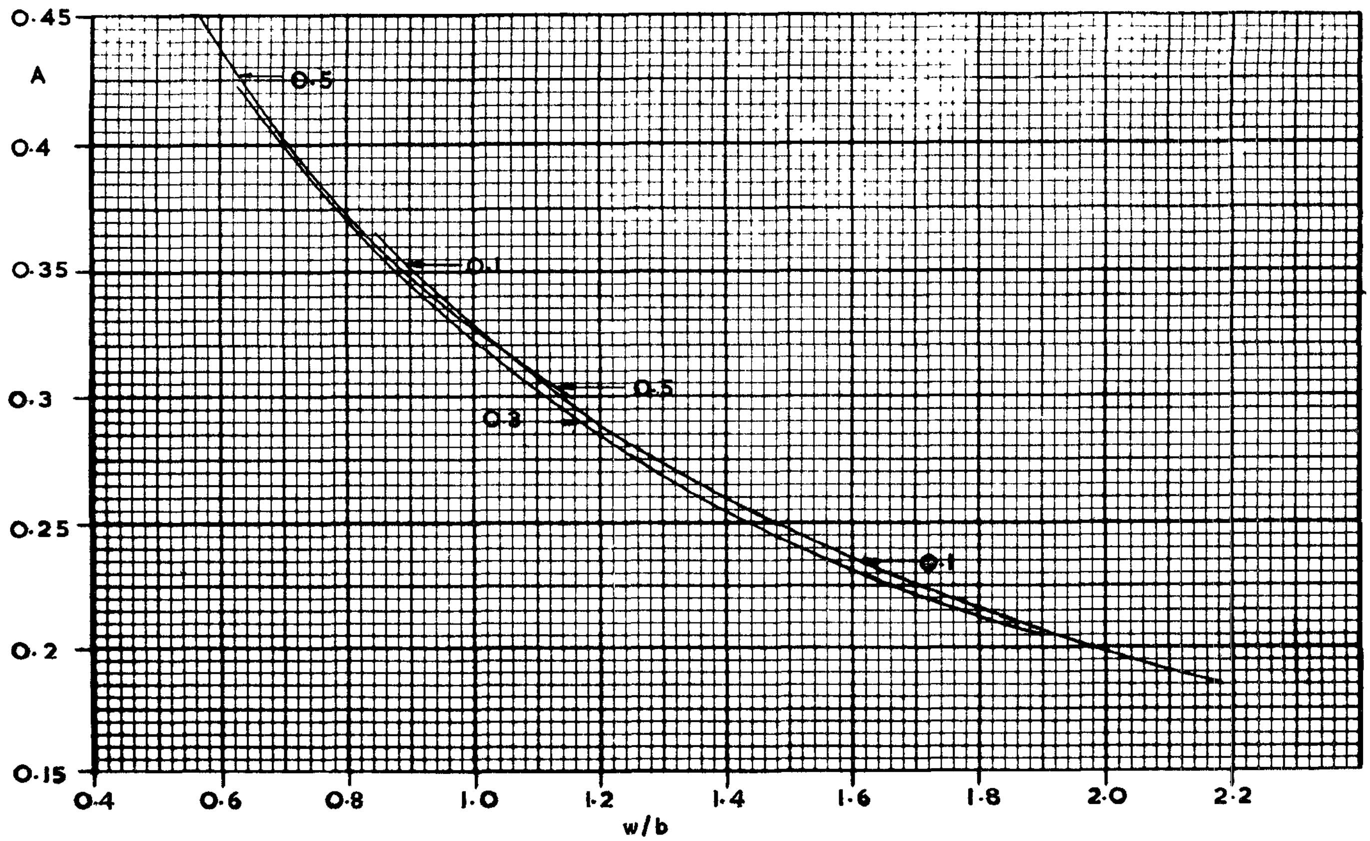

Fig. 7—The constant A of the frequency-shift formulas, as a function of w/b, with t/b as parameter.

$$\frac{\delta\omega}{\omega} + \frac{j}{2}\left[\frac{1}{Q_1} - \frac{1}{Q_0}\right] = \frac{-(\epsilon - 1)E_0^2 V_1}{\frac{1}{2}\cdot 4E_0^2 V_0}$$

where E_0^2 means the value at the sample position, and the factor 1/2 arises from the sinusoidal variation of electric field along the cavity. Then

$$\frac{\delta\omega}{\omega} + \frac{j}{2}\left[\frac{1}{Q_1} - \frac{1}{Q_0}\right] = \frac{-(\epsilon - 1)}{2}\cdot\frac{x\cdot 2l_1}{l_0}\cdot$$

We require the result in terms of y rather than x. Taking y to be the mean of (53), and substituting for λ from (22), we obtain

$$\frac{\delta\omega}{\omega} + \frac{j}{2}\left[\frac{1}{Q_1} - \frac{1}{Q_0}\right] = -A(\epsilon - 1)\cdot\frac{2yl_1}{l_0} \qquad (55)$$

where

$$A = \frac{\pi\alpha}{2(\alpha + \beta)K(1/\alpha)}\sqrt{\frac{\alpha^2 - \beta^2}{\alpha^2 - 1}}\cdot \qquad (56)$$

A is given graphically as a function of w/b, with t/b as a parameter, in Fig. 7. The real and imaginary parts of (55) then give the real and imaginary parts of ϵ in terms of the frequency shift and change of Q, respectively.

It is evident that the sample need not be in the form of a rectangular block. What is important is that its height be equal to the separation between strip and ground plane, and that its section perpendicular to this dimension be constant. Then, for any other cross section than the rectangular section we have been considering, $2yl_1$ is to be replaced by the half-area of the section. For the same accuracy, the dimensions of the area of the section must not exceed $2y$ or $2l_1$.

The accuracy of (55) depends on the assumption that the field in which the sample is placed is uniform. Because it is not, the value of the numerator of the perturbation formula will be slightly less than the value we have calculated. We consider separately the errors due to finite l_1 and finite y.

Because l_1 is finite, the field at the end of the sample, which we have taken to be E_0, is in fact $E_0 \cos \xi$, where $\xi = \pi l_1/l_0$. The error is due to the difference between the integral of $E_0^2 \cos^2 \xi$ over l_1 and the integral of E_0^2. Thus the fractional error is found to be $\pi^2 l_1^2/3l_0^2$. In performing an experiment, the sample must be designed so that

$$\frac{100\pi^2 l_1^2}{3l_0^2} < \text{tolerable percentage error}$$

or, if the error is to be less than f per cent,

$$l_1/l_0 < 0\cdot055\sqrt{f} \qquad (57)$$

for a half-wave cavity. For a longer cavity, replace l_0 by $\lambda_0/2$ in this formula.

The limitation on y is due to the terms in x^3 in (43) and (44). For a thin layer of the sample near QA, the energy distribution goes as $E_0^2[1 - K^2x^2(1 - \beta^2/\alpha^2)]$ instead of E_0^2. On integrating over the range 0 to y, the fractional error in the perturbation due to this element is found to be, analogously to the above calculation for the effect of finite l_1,

$$\frac{\pi^2 y^2(\alpha^2 - \beta^2)^2}{3b^2(\alpha + \beta)^2(\alpha^2 - 1)}.$$

Similarly, for an element near RB, the fractional error is

$$\frac{\pi^2 y^2(\alpha^2 - \beta^2)^2}{3\alpha\beta b^2(\alpha + \beta)^2(\alpha^2 - 1)}.$$

These expressions are nearly equal when α and β are near to unity, and are then very small even for large values of y/b. They are of opposite sign, so that these errors tend to cancel, and the over-all fractional error is, therefore, smaller than either of these expressions. It is likely that a bigger error would be given by the term in x^5, for it seems reasonably certain that the error should increase considerably as the sample enters into the fringing fields. We therefore conclude, tentatively, that for accurate results $y^4/b^4 \ll 1$. For 1 per cent accuracy, this would allow y/b to be of the order of 0.3. We expect that y/w would also be significant, but w usually will not be much less than b, so that we may equally well write $y^4/w^4 \ll 1$.

V. Measurement of Magnetic Properties

For these measurements, the ferrite sample is to be placed at the end of the cavity, flush with the end wall. We shall assume a single sample, *i.e.*, on one side only of the strip. The sample dimension parallel to the axis of the cavity is l_1, that perpendicular to the axis and parallel to the plane of the strip is again $2y$, and the vertical dimension may be either $b-t$ or a quantity s. There are three cases. In all cases, the polarizing field is vertical, *i.e.*, perpendicular to the ground planes.

Case 1) The sample is a flat rectangular plate on the end wall. The height is $b-t$, so that the ends are flush with the ground plane and the strip, and $l_1 \ll y$.

Case 2) The sample is a flat plate with its plane perpendicular to the end wall and to the strip. The height is again $b-t$, and $y \ll l_1$, $y \ll (b-t)$.

Case 3) The sample is a flat plate lying on the strip, with thickness s. We require $s \ll l_1$ and $s \ll y$.

The effect of placing the sample against the end wall is to reflect it in the wall; this doubles the effective size of the sample, but also doubles the effective size of the cavity. Thus a half-wave cavity with a sample of length l_1 against its end is, to the extent to which the end can be regarded as perfectly conducting, equivalent to a full-wave cavity with a sample of length $2l_1$ at its center.

For case 1) the external microwave magnetic field is parallel to the plane of the plate and we

$$\boldsymbol{H}_0 \cdot \boldsymbol{B}_1 - \boldsymbol{H}_1 \cdot \boldsymbol{B}_0 = \mu_0 H_0^2(\mu - 1 - \alpha^2/\mu),$$

while for case 2) the microwave magnetic field is perpendicular to the plane of the plate, and

$$\boldsymbol{H}_0 \cdot \boldsymbol{B}_1 - \boldsymbol{H}_1 \cdot \boldsymbol{B}_0 = \mu_0 H_0^2(1 - 1/\mu).$$

For case 3), we find

$$\boldsymbol{H}_0 \cdot \boldsymbol{B}_1 - \boldsymbol{H}_1 \cdot \boldsymbol{B}_0 = \mu_0 \boldsymbol{H}_0^2(\mu - 1).$$

We substitute into the perturbation formula and proceed as in Section IV. The results are:

Case 1)

$$\frac{\delta\omega}{\omega} + \frac{j}{2}\left[\frac{1}{Q_1} - \frac{1}{Q_0}\right] = -A(\mu - 1 - \alpha^2/\mu)\cdot\frac{yl_1}{bl_0}. \quad (58)$$

Case 2)

$$\frac{\delta\omega}{\omega} + \frac{j}{2}\left[\frac{1}{Q_1} - \frac{1}{Q_0}\right] = -A(1 - 1/\mu)\cdot\frac{yl_1}{bl_0}. \quad (59)$$

Case 3)

$$\frac{\delta\omega}{\omega} + \frac{j}{2}\left[\frac{1}{Q_1} - \frac{1}{Q_0}\right] = -B(\mu - 1)\cdot\frac{yl_1 s}{bl_0(b - t)}. \quad (60)$$

Here A is the same constant as in (56) and is given by Fig. 7. For case 3), the sample is close to RS of Fig. 1, so we use the second of expressions (53) for the relation between y and x, instead of the mean. Then

$$B = (1 + \beta/\alpha)(A/2) \quad (61)$$

and B can be obtained from the curve of Fig. 7 by evaluating α and β from w/b and t/b with the aid of Figs. 4 and 5.

The limitations on y and l_1 for a given desired accurary are the same as in the dielectric case, so no further discussion is necessary. The inherent error arising from the geometry of the cavity is also the same as in the dielectric case, for cases 1) and 2), but does not arise in case 3).

Samples may also be used in the form of plates which may not be rectangular, and the frequency shift will be proportional to the area, so that in case 1) the frequency-shift formula is obtained by multiplying the right-hand side of (58) by $S/y(b-t)$ where S is the area of the sample. For case 2), multiply the right-hand side of (59) by $S/l_1(b-t)$, and for case 3) multiply the right-hand side of (60) by S/yl_1. When these alterations are made, the area S must lie within the limits for y and l_1 if the same accuracy in the frequency-shift formula is to be obtained. Also, the sample must still fit flush against the end wall; the reason for this is discussed by Waldron.[5]

By making a measurement using case 1), and another measurement using either case 2) or case 3), μ and α can be separately determined if required. The gyromagnetic-resonance linewidth can be obtained from observations of the change of Q, using any of cases 1), 2) and 3), for the linewidth of $1/Q$ can be shown to be equal to the linewidth of the permeability in all three cases.

VI. Summary and Discussion

Measurements of dielectric constants of samples in the form of rectangular blocks can be made by placing

[5] R. A. Waldron, "Ferrites: An Introduction for Microwave Engineers," D. Van Nostrand Company, Princeton, N. J., pp. 119–121; 1961.

the sample at the center of the cavity as shown in Fig. 6. The relation between frequency shift and dielectric constant is then given by (55), using the value of A obtained from Fig. 7 or (56).

There is a limitation on the accuracy achievable with a given cavity, due to the form of the fields near the axis. This limiting accuracy is indicated in Figs. 4 and 5 by the dashed curves. From these diagrams, the limiting value of accuracy obtainable for given values of w/b and t/b can be read off. When designing a cavity, this question must be considered.

The accuracy of an experiment is also dependent on the extent to which the assumption is valid that the field in the neighborhood of the sample is uniform. If the error due to the finite length $2l_1$ of the sample is not to exceed f per cent, the limitation on l_1 is given by (57). It is difficult to estimate the error due to the finite value of y, because, on expanding a certain expression as a power series in y, the coefficient of the second term turns out to be very small, so that it is likely that the error due to the third term will be the significant one. This suggests a tentative requirement that y^4/b^4 and y^4/w^4 be very small compared with unity.

It is not necessary that the horizontal section of the sample be rectangular, as long as the sides are vertical and the sample height is $b-t$. The area $4yl_1$ of the rectangular sample is then to be replaced by the area of the sample actually being used. For the same accuracy as with a rectangular sample, the greatest horizontal dimensions should not exceed $2y$ and $2l_1$.

For measurements of the elements of the permeability tensor of a ferrite, the sample should be in the form of a thin flat rectangular plate. This may be placed with its plane vertical, perpendicular to the end wall [case 2)]; or with its plane horizontal, against the live strip [case 3)]. By making another measurement, with the sample against the end wall [case 1)], both the diagonal and the off-diagonal elements can be obtained. In case 2) and 3), one edge of the plate lies against the end wall. The formulas for the freqency shifts are given in (58)–(60). The same considerations of errors apply as in the dielectric case, except that in case 3) there is no inherent error in the cavity design because the sample does not occupy the full height of the cavity.

In designing a cavity, the dimensions w, b, and t have to be chosen to give suitable values of Q, of the constant A of (55), and of the inherent error in the cavity due to the finite departures of α and β from unity. These quantities must be considered in relation to the values of the properties to be measured, the accuracy desired, the practical limitations there may be on the size of sample that can be made, and the accuracy with which the frequency shift and change of "Q" can be measured with the gear available. The constant A can be read off from Fig. 7. The "Q" of a cavity is given by (52).

Symbols

l_0 = Length of the cavity.

b = Half the distance between the ground planes.

t = Half the thickness of the live strip.

w = Half the width of the strip.

α, β, λ = Parameters used in the mapping, and related to w, t, and b by (19)–(22). See also Figs. 4 and 5.

$\beta' = \sqrt{1-\beta^2}$.

$\gamma = \sqrt{1-1/\alpha^2}$.

F, Π = Elliptical integrals of the first and third kinds, respectively.

K = Complete elliptic integral of the first kind.

$\boldsymbol{E}_0$, $\boldsymbol{D}_0$, $\boldsymbol{H}_0$, $\boldsymbol{B}_0$ = Fields and inductions in the cavity in the unperturbed condition.

$\boldsymbol{E}_1$, $\boldsymbol{D}_1$, $\boldsymbol{H}_1$, $\boldsymbol{B}_1$ = Fields and inductions which must be added to $\boldsymbol{E}_0$, $\boldsymbol{D}_0$, $\boldsymbol{H}_0$, and $\boldsymbol{B}_0$, to give the fields and inductions in the cavity in the perturbed condition.

ϵ_0, μ_0 = Permittivity and permeability of free space.

ϵ = Dielectric constant of material under test.

μ, α = Diagonal and off-diagonal element of relative permeability tensor of ferrite under test.

σ = Conductivity of the cavity walls.

δ = Skin depth of the material of the cavity walls.

Q = Quality factor.

Q_0 = "Q" of the cavity in the absence of a sample.

Q_1 = "Q" of the cavity when it contains a sample.

V_0 = Cavity volume.

V_1 = Volume over which a change in properties is made, *i.e.*, the whole of space external to V_0 in Section III, and the sample volume in Sections IV and V.

$\omega = 2\pi$ times resonance frequency of the cavity.

λ_0 = Free-space wavelength corresponding to ω.

x = The ratio of QA to QP in Fig. 3.

y = Half the width of the sample (parallel to w).

l_1 = Half the length of the sample for a dielectric measurement, or the whole length for a magnetic measurement (parallel to l_0).

s = Height of the sample in case 3 of the magnetic measurement (parallel to b).

A = Numerical constant occurring in the frequency-shift expressions. It is given by (56) and plotted in Fig. 7.

Acknowledgment

The author wishes to thank Miss S. P. Maxwell for suggesting the problem, B. Westcott for assistance with the computations, Dr. R. J. Benzie for his interest in the work, and the Director of Research of The Marconi Company for permission to publish this paper.